



*Supplement of*

## **Recent and projected changes in rain-on-snow event characteristics across Svalbard**

**Hannah Vickers et al.**

*Correspondence to:* Hannah Vickers ([havi@norceresearch.no](mailto:havi@norceresearch.no))

The copyright of individual parts of the supplement might differ from the article licence.

## Supplementary Material

To demonstrate model uncertainty in the discussion of the HCLIM km-scale climate projections, and broaden our range of possible future climate change outcomes in Svalbard and the wider Arctic, we have analysed spatially coarser projections downscaled from two other CMIP6 models that were chosen to represent much of the spread in CMIP6 climate projections for the extended summertime Arctic (Levine *et al.*, 2024). These high resolution Arctic climate simulations were developed using a storylines approach (Shepherd *et al.*, 2018) in the EU-funded PolarRES project. The GCM projections that were chosen for dynamical downscaling are CNRM-ESM2-1 and NorESM2-MM, which represent two diametrically opposing storylines, thus capturing much of the spread in projected changes for the extended Arctic summer. Whereas CNRM-ESM2-1 represents weak Arctic amplification and strong Barent-Kara sea warming, NorESM2-MM represents strong Arctic amplification and weak Barents-Kara sea warming. Including simulations representing these storylines facilitates a better representation of the range of plausible outcomes of future climate change for the region of study.

Like MPI-ESM1-2-LR, these two GCMs were also downscaled using the HCLIM model system, but in a hydrostatic configuration using HCLIM-ALADIN physics (also described in Belušić *et al.* 2020 and Wang 2024) and with a coarser 11 km horizontal grid spacing. The model setup is otherwise mostly identical to that which was described in section 2.3: HCLIM climate model data. From hereon the HCLIM simulations produced by downscaling the NorESM and CNRM with HCLIM will be referred to as HCLIM11-NorESM and HCLIM11-CNRM respectively. ROS days are detected using the same thresholding approach described in section 2.3 in the main text.

Similar to the evaluation of the present climate conditions using the HCLIM-downscaled ERA5 dataset at 2.5km, we have also evaluated a dynamical downscaling of ERA5 with HCLIM for the same domain at a resolution of 11 km for the period 2000-2020. The results are compared with HCLIM-ERA5 dataset at 2.5km in Figure S1. Examining the 11km HCLIM-ERA5 mean ROS characteristics in Fig.S1 (e) to (h) and the differences with the CARRA means in Fig.S1 (m) to (p) it is clear that despite the lower spatial resolution the 11km HCLIM-ERA5 dataset reproduces the overall present-day climatology remarkably well, with absolute values very similar to those of the higher resolution 2.5km HCLIM-ERA5 dataset shown in Fig.S1(a) to (d). The greatest deviations from the CARRA means are typically the result of the 11km HCLIM-ERA5 dataset not being able to resolve smaller lowland valleys for example those found across Nordenskiöld Land.

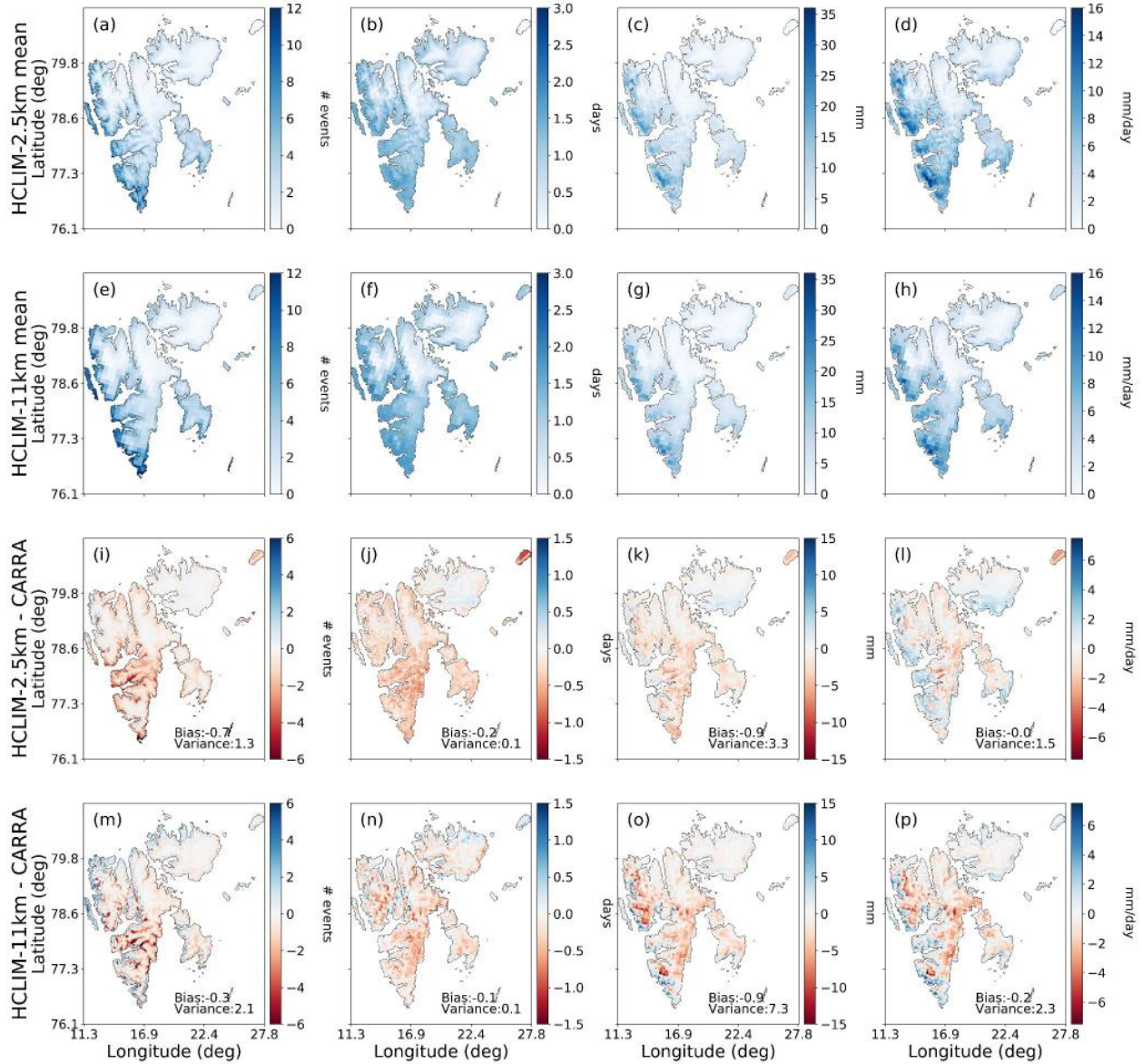


**Figure S1: ROS climatology for 2000-2020 obtained with HCLIM-ERA5 at 2.5km resolution (a to d) and HCLIM-ERA5 at 11km resolution (e to h) and the differences between HCLIM-ERA5 (2.5km) and CARRA (i, to l) and HCLIM-ERA5 (11km) and CARRA for the 2000-2020 period (m to p).**

### HCLIM11-CNRM projections

In Figure S2 the projected change in the mean number of ROS events, the mean duration, total precipitation, and intensity in the 2030-2050 and 2050-2070 periods from the HCLIM11-CNRM dataset at 11km resolution, compared to the mean for the historical period (2000-2020) is shown. This set of projections, corresponding to strong warming in the Barents-Kara Sea, and a relatively weak Arctic amplification, depicts a contrasting future scenario for ROS compared to the HCLIM-MPI dataset; in this set of projections, reductions in all of the ROS characteristics are projected to be widespread across the archipelago in both the 2030-2050 period and 2050-2070 period. In particular the east coast of Spitsbergen stands out as an area that may experience the greatest reduction in ROS duration, total precipitation and intensity in 2030-2050, while ROS events could decrease most in the southwest of the archipelago

and across Edgeøya for this period with respect to the 2000-2020 period. In contrast there is projected to be little change in ROS events over the whole archipelago in the later 2050-2070 period compared to 2000-2020, indicating that after an initial decrease between 2030-2050 ROS events may start to increase again in the southwest and east of the archipelago. Only in the coastal parts of Nordaustlandet are there projected to be small increases in all of the ROS characteristics in both future periods, but these changes become more prominent when expressed as a relative change (percentage of the present-day values) as shown in Figure S3. This figure also shows that a “hotspot” of large increases in all ROS characteristics relative to the present-day values is found in the northern part of Spitsbergen just west of Nordaustlandet.

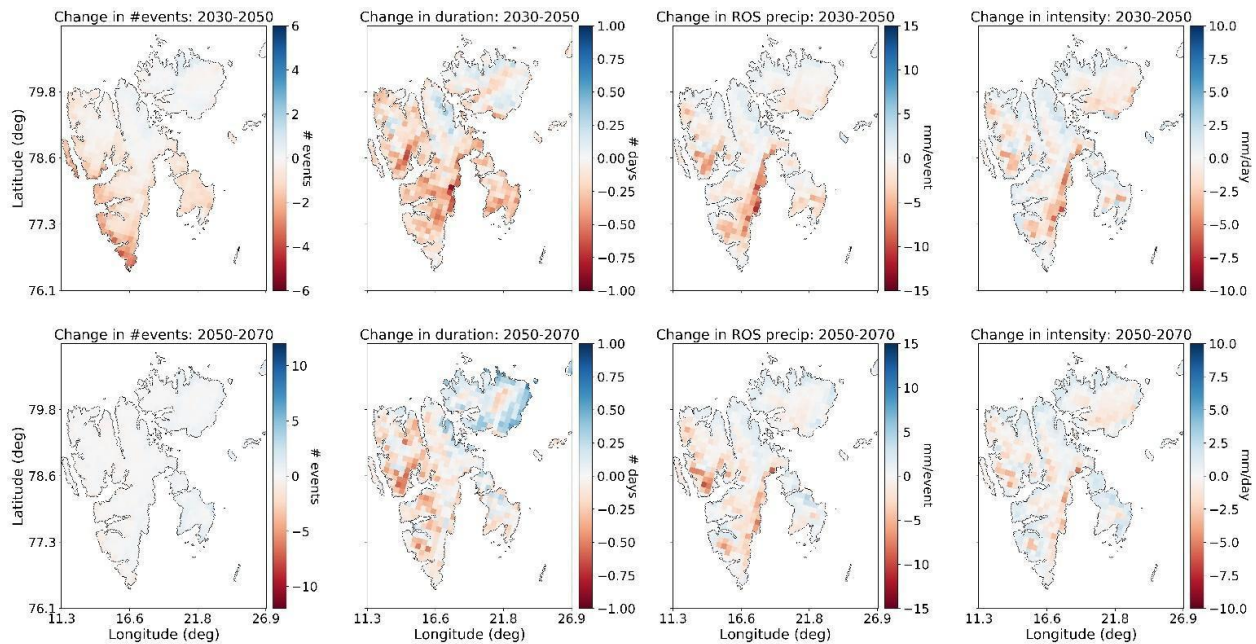


**Figure S2: Change in ROS frequency, duration, total precipitation, and mean intensity for 2030-2050 (upper row) and 2050-2070 (lower row) relative to the 2000-2020 averages obtained using the HCLIM11-CNRM 11km projections.**

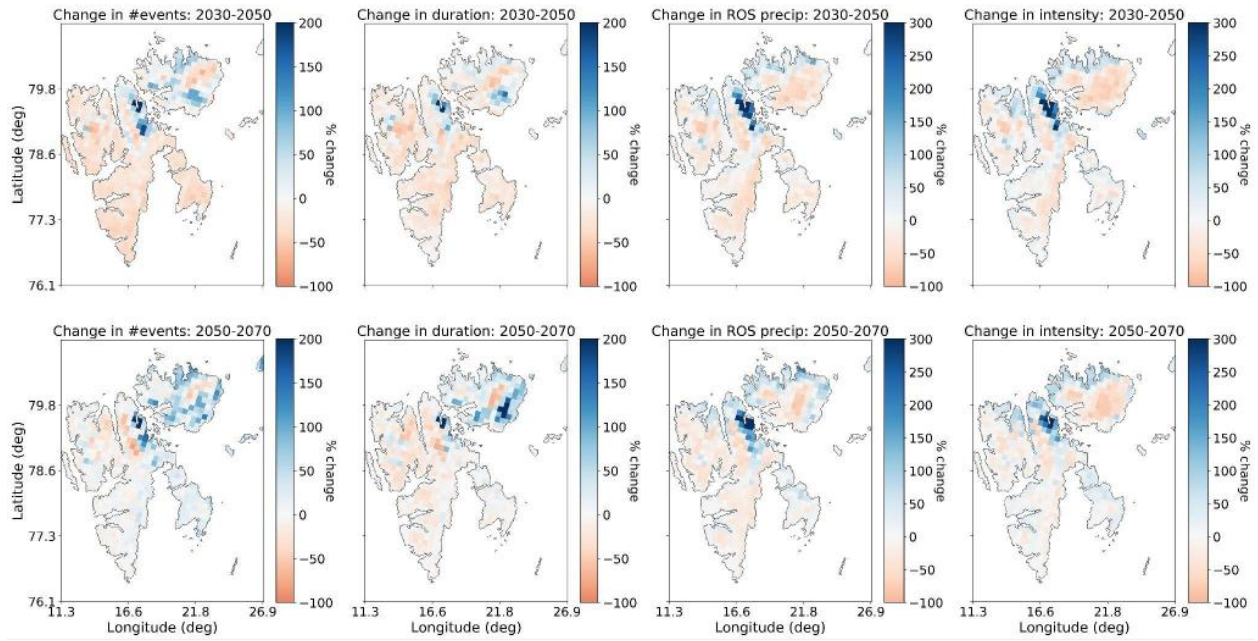


**Figure S3: The relative change in ROS frequency, duration, total precipitation, and mean intensity for 2030-2050 (upper row) and 2050-2070 (lower row) relative to the 2000-2020 averages obtained using the HCLIM11-CNRM 11km projections**

When examining the changes in ROS events by month for the 2030-2050 period in Figure S4, there is a clear pattern of reduction in ROS frequency across all of the archipelago except the northernmost part of Nordaustlandet in October and November, while in mid-winter and late spring the reduction in ROS events becomes confined to predominantly the western and southern parts of the archipelago (January to March and May). Only in April for both future periods will ROS frequency not change much with respect to the present climate. For the later 2050-2070 period there is a more mixed picture of change, with October and February still exhibiting mostly reductions in ROS frequency, while in November and March there are projected to be small increases in ROS frequency across the southern parts of Spitsbergen and Edgeøya. Overall, the change in ROS frequency for 2050-2070 is smaller in all months compared to the projected change for 2030-2050.

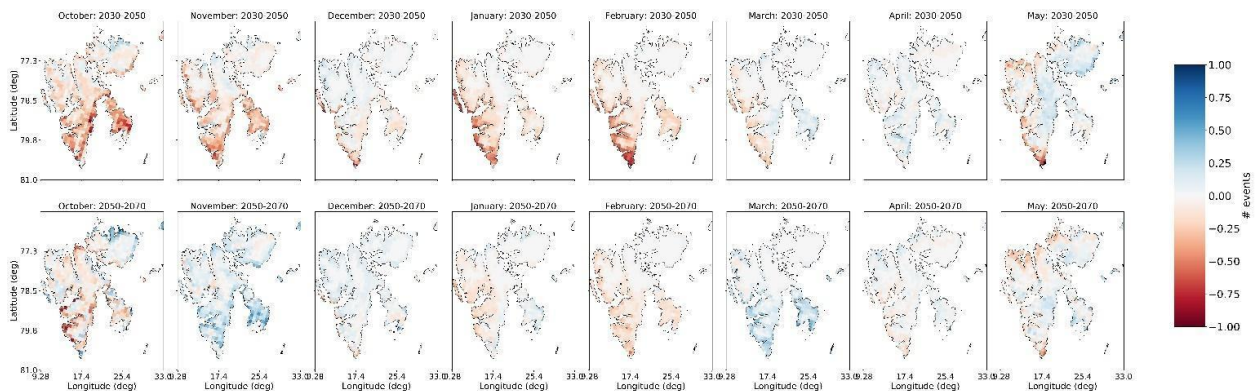


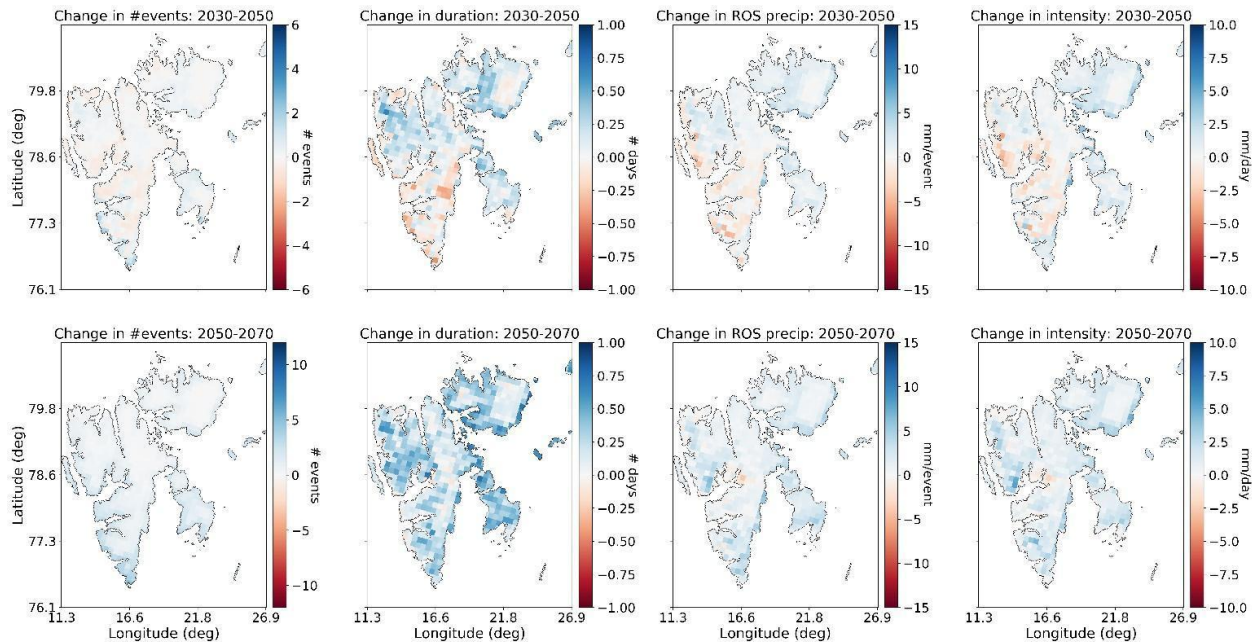
**Figure S4: Changes in ROS frequency by month from October to May, for 2030-2050 (upper row) and 2050-2070 relative to the reference period 2000-2020 obtained using the HCLIM-downscaled CNRM dataset.**



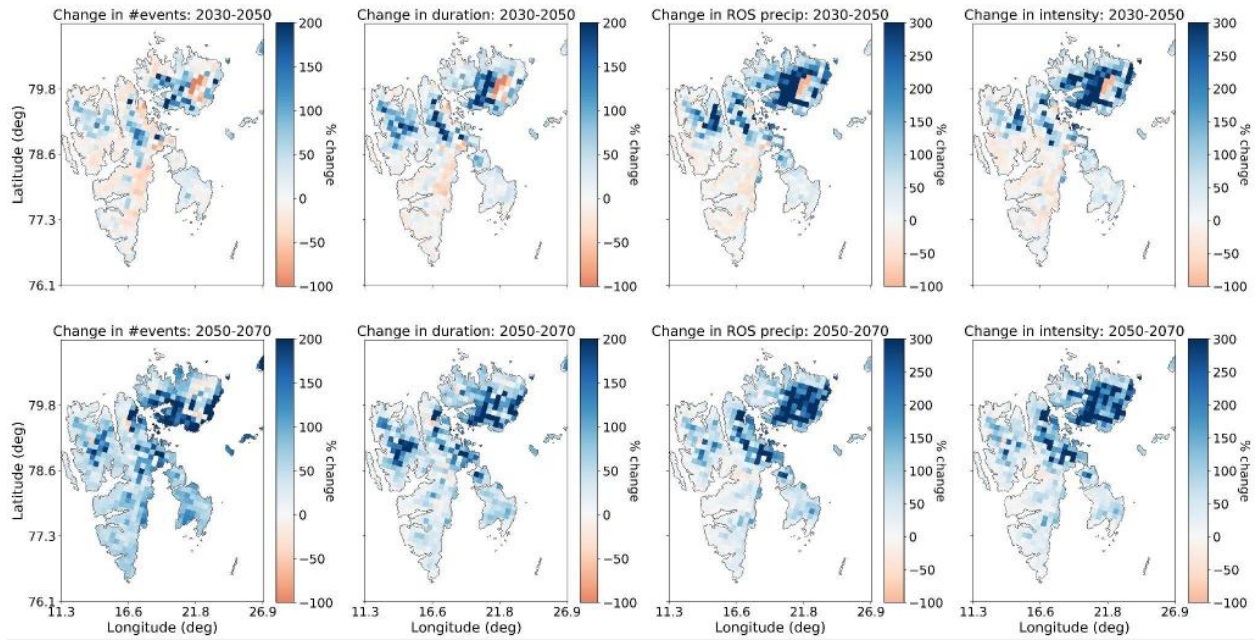
## HCLIM11-NorESM 11km projections

Figure S5 shows the changes in the four ROS characteristics using the HCLIM-downscaled NorESM climate projections. The downscaled NorESM projections share some similarities with the downscaled MPI datasets; like the HCLIM-MPI projections (Fig.4, main text), the HCLIM11-NorESM projections show a reduction in the ROS characteristics in the western and southern parts of the archipelago but increases in the north and east. On the other hand, there will be relatively overall minor changes in ROS frequency compared to the large increases projected by HCLIM-MPI. Moreover, whereas HCLIM-MPI projects significant increases in ROS duration over the high lying inner parts of Nordaustlandet and northern Spitsbergen in the 2050-2070 period, the HCLIM11-NorESM projections show that these areas will experience the smallest change in ROS duration compared to coastal parts of Nordaustlandet and Spitsbergen. Areas that were projected to experience small reductions in ROS total precipitation and intensity in the 2030-2050 period, such as southern, western and central Spitsbergen, are projected to have increases in these same characteristics relative to the 2000-2020 period, by 2050-2070.

The changes expressed as a percentage of the present-day values, shown in Figure S6 show a similar pattern of change to those projected by HCLIM-MPI. The high lying northern areas of Spitsbergen and Nordaustlandet stand out as those areas that could have the largest increases in all ROS characteristics in both future periods, with a relative change more than 300%. The HCLIM-MPI projections suggest a relative change of 400-500% for these areas, so there is some agreement in the magnitude and location of the greatest changes despite the more aggressive emissions scenario of the MPI dataset.



**Figure S5: Change in ROS frequency, duration, total precipitation, and mean intensity for 2030-2050 (upper row) and 2050-2070 (lower row) relative to the 2000-2020 averages obtained using the HCLIM11-NorESM 11km projections.**



**Figure S6: Change in ROS frequency, duration, total precipitation, and mean intensity for 2030-2050 (upper row) and 2050-2070 (lower row) expressed as a percentage of the 2000-2020 averages obtained using the HCLIM11-NorESM dataset**

For the monthly changes, Figure S7 shows that the HCLIM11-NorESM projections are almost opposite to those of the HCLIM11-CNRM dataset. Whereas HCLIM11-CNRM projects a drier October and a very slight increase in ROS in April, HCLIM11-NorESM projects increases in ROS events in both October and May and a reduction in ROS events in April, in both future periods. It may be recalled that HCLIM-MPI also projected increases in ROS in most months for both future periods, with only the westernmost coastal regions having projected decreases in ROS events in October and May. The near-future period (2030-2050) shows opposite patterns of change in November, December and February compared to the later 2050-2070 in the HCLIM11-NorESM projections; in 2030-2050 there are projected small decreases in ROS events in these months over large parts of the archipelago relative to the present climate, whereas in 2050-2070 there are projected to be increases in ROS events. In general, the magnitude of change in the 2050-2070 period is greatest in the coastal regions of Spitsbergen, Nordaustlandet and Edgeøya in October and May when compared with all other months.

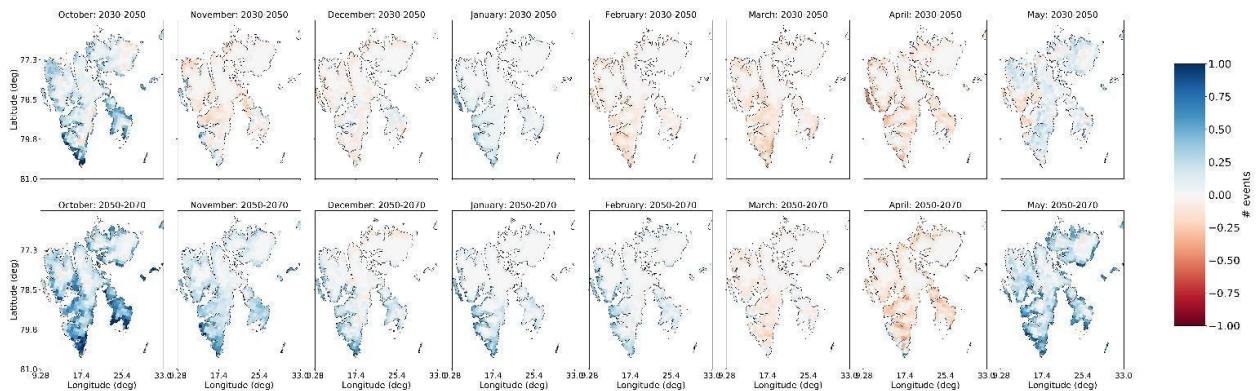


**Figure S7: Changes in ROS frequency by month from October to May, for 2030-2050 (upper row) and 2050-2070 relative to the reference period 2000-2020 obtained using the HCLIM-downscaled NorESM dataset.**

In Figure S8 we have combined the results from the HCLIM-MPI projections with the HCLIM11-CNRM and HCLIM11-NorESM projections to show only areas where all three models were in agreement on the sign of change (i.e. positive or negative). As indicated by the large proportion of grey-colored areas, the future change in the four ROS characteristics is uncertain across a large part of the archipelago, especially in the 2030-2050 period. However, all three models agree for example, that there will be a reduction in ROS duration, total precipitation and intensity in the western parts of Spitsbergen and increases in all characteristics across coastal and northern parts of Nordaustlandet. In the later 2050-2070 period, there are greater areas of the archipelago where the three model projections agreed over the sign of change in each of the four characteristics. For ROS frequency in particular, all three models projected an increase for predominantly the eastern and northern parts of Svalbard, including much of Edgeøya. For ROS duration, total precipitation and intensity the models agreed over increases in the northern and northeastern parts of Svalbard, as well as Edgeøya in the 2050-2070 period.

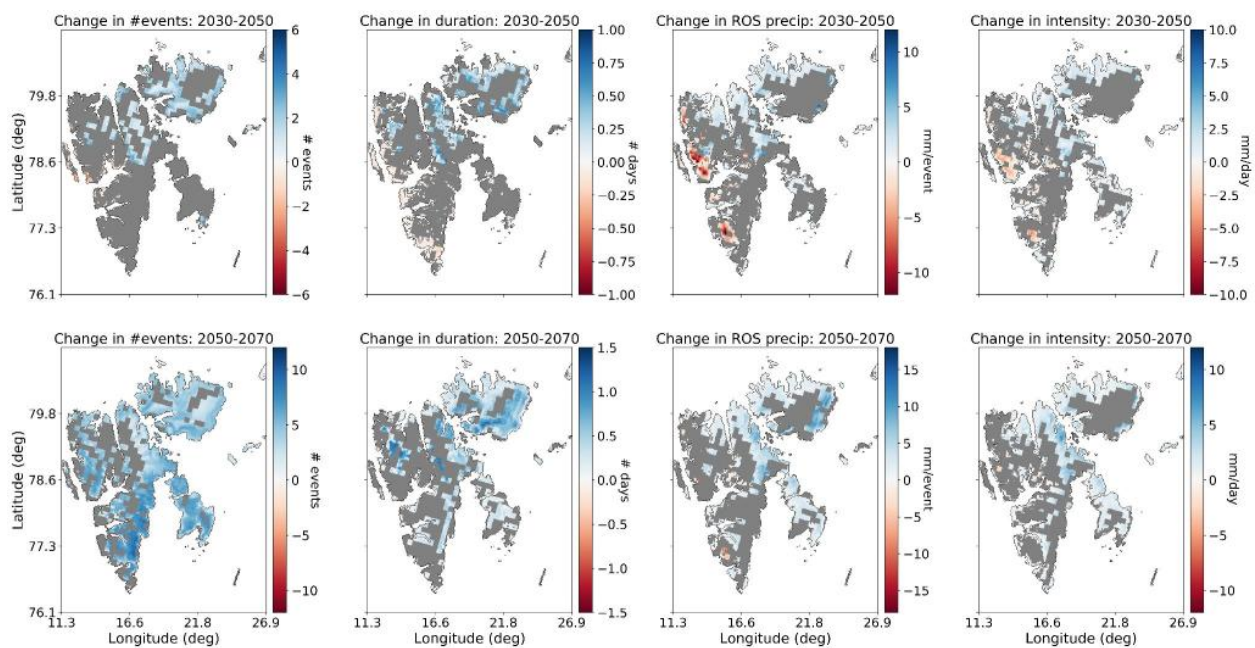


**Figure S8: Change in ROS frequency, duration, total precipitation, and mean intensity for 2030-2050 (upper row) and 2050-2070 (lower row) using the HCLIM-MPI projections. Grey areas correspond to grid cells where the three sets of projections did not agree on the sign of the change and the data value has been masked out.**